

A spin-crossover iron(II) coordination polymer with the 8-aminoquinoline ligand: synthesis, crystal structure and magnetic properties of $[\text{Fe}(\text{aqin})_2(4,4'\text{-bpy})](\text{ClO}_4)_2 \cdot 2\text{EtOH}$ (aqin = 8-aminoquinoline, 4,4'-bpy = 4,4'-bipyridyl)[†]

Caroline Genre,^a Galina S. Matouzenko,^{*a} Erwann Jeanneau^b and Dominique Luneau^b

Received (in Montpellier, France) 19th June 2006, Accepted 24th July 2006

First published as an Advance Article on the web 31st August 2006

DOI: 10.1039/b608679a

We report here on the synthesis and characterisation of a new iron(II) spin-crossover coordination polymer of formula $[\text{Fe}(\text{aqin})_2(4,4'\text{-bpy})](\text{ClO}_4)_2 \cdot 2\text{EtOH}$ (aqin = 8-amino-quinoline, 4,4'-bpy = 4,4'-bipyridyl), with a linear chain structure. Variable temperature magnetic susceptibility measurements revealed a relatively abrupt HS \leftrightarrow LS spin transition, with $T_{1/2} = 220$ K (temperature for which the HS fraction is equal to 0.5). The crystal structure was resolved at 293 K (HS form) and 80 K (LS form). Both spin state structures belong to the monoclinic space group $C2/c$ ($Z = 4$). The complex assumes a one-dimensional linear chain structure, in which the active iron(II) sites are linked to each other by rigid rodlike 4,4'-bipyridyl molecules acting as chemical bridges. The Fe–Fe distance through the 4,4'-bpy ligand is 11.485 and 11.147 Å in the high-spin and low-spin structures, respectively. The polymeric chains extend in the b direction and form sheets parallel to the bc plane. They are linked together by π -stacking interactions and H-bonding between the H-donor aqin ligands and the perchlorate ions. Those structural features provide a basis for cooperative interactions.

Introduction

The design and characterisation of new molecular compounds exhibiting spin-crossover behaviour is one of the most relevant and challenging questions in the field of magnetic materials chemistry.^{1,2} Iron(II) compounds have been extensively studied in the last decades, for they are liable to show a temperature induced LS \leftrightarrow HS ($^1A_1 \leftrightarrow ^5T_2$ in octahedral geometry) transition. Their bistability makes them suitable for use in molecular scale electronic devices, such as memories or displays, where a quick switch between two states is needed.³ Those potential applications require an abrupt spin transition, with a relatively large thermal hysteresis, centered near ambient temperature. The steepness of the spin transition in a solid depends on the cooperativity between the metal sites, that is to say the ability of the crystal lattice to efficiently transmit the electronic features and the geometry changes that occur in the iron coordination sphere upon spin conversion from one molecule to another.⁴ Different intermolecular interactions (π -stacking, hydrogen bonding, van der Waals interactions) are thought to play a role as information transmitters. However, those are non-covalent interactions and their spreading

in the crystal is difficult to control.⁵ Olivier Kahn *et al.* first introduced the idea that direct covalent linking of the active metal sites through chemical bridges could improve cooperativity in polymeric compounds in regard to mononuclear ones.⁶ Rodlike spacers like 4,4'-bipyridyl have allowed the engineering of numerous metal-containing polymers with a large diversity of network topologies, such as one-dimensional molecular chains and ladders, two-dimensional grids and brick-wall structures and three-dimensional frameworks.⁷ These coordination polymers are of high interest because of their promising catalytic, electrical, optical and magnetic properties.^{7,8} However, only a few iron(II) polymeric spin-crossover compounds have been reported so far.^{9–25}

In this connection we attempted to synthesise new polymeric spin-crossover systems by self-assembly of nitrogenated organic molecules involving mixed aliphatic, aromatic and imidazolic functions and metal ion building blocks. Our approach consists of trying to gain cooperativity between the metal sites through combining the efficiency of the rigid 4,4'-bipyridyl spacer at propagating geometry changes with the ability of ligands containing amine functions to create H-bond networks with counter-ions or solvent molecules within the crystal. In this paper we report the synthesis, structure and magnetic properties of the novel spin transition complex $[\text{Fe}(\text{aqin})_2(4,4'\text{-bpy})](\text{ClO}_4)_2 \cdot 2\text{EtOH}$ with aqin = 8-aminoquinoline and 4,4'-bpy = 4,4'-bipyridyl. This compound exhibits a relatively sharp LS \leftrightarrow HS transition centered around $T = 220$ K. It forms linear chains which are linked together *via* H-bonding and π -stacking interactions. Only two linear spin-

^a Laboratoire de Chimie (UMR CNRS and ENS Lyon n5182), Ecole Normale Supérieure de Lyon, 46, allée d'Italie, 69364 Lyon Cedex 07, France. E-mail: Galina.Matouzenko@ens-lyon.fr

^b Laboratoire des Multimatériaux et Interfaces (UMR CNRS n5615), Université Claude Bernard Lyon-1, 69622 Villeurbanne Cedex, France

[†] The HTML version of this article has been enhanced with colour images

crossover polymers have been characterised by X-ray crystallography until now^{14,18} However in both these examples the transitions are incomplete and much less cooperative than in the presented complex.

Experimental

Materials

$\text{Fe}(\text{ClO}_4)_2 \cdot 6\text{H}_2\text{O}$, 8-aminoquinoline (aqin) and 4,4'-bipyridyl (4,4'-bpy) were purchased from Aldrich Chemical Co. and used as received. The synthesis was carried out in deoxygenated solvent under an inert atmosphere of N_2 using glovebox techniques. Elemental analyses (C, H and N) were performed by the Service Central d'Analyses du CNRS in Vernaison, France.

Synthesis of the complex $[\text{Fe}(\text{aqin})_2(4,4'\text{-bpy})](\text{ClO}_4)_2 \cdot 2\text{EtOH}$

A total of 72.6 mg (0.2 mmol.) of $\text{Fe}(\text{ClO}_4)_2 \cdot 6\text{H}_2\text{O}$ was dissolved in 3 mL of ethanol, and 31.2 (0.2 mmol) mg of 4,4'-bpy in 2 mL of ethanol was added. A light yellow solution was formed. The addition of 57.6 mg (0.4 mmol) of aqin in 3 mL of ethanol turned this solution to an intense orange-red. The solution was filtered and allowed to stand overnight at room temperature, to give red crystals of $[\text{Fe}(\text{aqin})_2(4,4'\text{-bpy})](\text{ClO}_4)_2 \cdot 2\text{C}_2\text{H}_5\text{OH}$, which were collected by filtration, washed with ethanol and dried under vacuum. The crystals used in the X-ray structure determination were selected from this sample (Found: C, 47.55; H, 4.17; N, 10.48. $\text{C}_{32}\text{H}_{36}\text{N}_6\text{O}_{10}\text{Cl}_2\text{Fe}$ requires C, 48.56; H, 4.59; N, 10.62%). Thermogravimetric analyses (temperature range: 25 to 135 °C, 2 °C per min) showed a weight loss of 11.82%, 11.62% being the expected value for two molecules of ethanol.

CAUTION: Perchlorate salts of metals with organic ligands are potentially explosive. Only small quantities of the compound should be prepared and handled with much care!

Physical measurements

Magnetic properties. Magnetic susceptibility measurements were carried out in the temperature range 80–300 K with a fully automated Manics DSM-10 susceptometer equipped with a TBT continuous cryostat and an electromagnet operating at 1.6 tesla. Data were corrected for diamagnetic contributions.

Solution and refinement of the X-ray structure. A Nonius Kappa CCD diffractometer using Mo $\text{K}\alpha$ radiation ($\lambda = 0.71069$ Å) and equipped with a CCD area detector was employed for data collection. A long time intensity data accumulation was tried using several non-protected or protected (Lindemann capillary or paratone oil) crystal samples. Due to low crystal stability, its transformation into a powder was observed after long enough irradiation. In order to avoid the crystal destruction, which was observed after 10 h, an optimal time for data measurement was adjusted. Intensities were collected at 80 K and 293 K by means of the program COLLECT²⁶ with a step rotation angle of 1 for the ω angle. Reflection indexing, Lorentz-polarisation correction, peak integration and background determination were carried out with the DENZO²⁷ program. Frame scaling and unit-cell para-

Table 1 Crystallographic data for $[\text{Fe}(\text{aqin})_2(4,4'\text{-bpy})](\text{ClO}_4)_2 \cdot 2\text{C}_2\text{H}_5\text{OH}$. Estimated standard deviations in the least significant digits are given in parentheses

	$T = 293$ K	$T = 80$ K
Empirical formula	$\text{C}_{32}\text{H}_{36}\text{Cl}_2\text{Fe}_1\text{N}_6\text{O}_{10}$	
M	791.435	
$a/\text{\AA}$	25.192(5)	24.531(5)
$b/\text{\AA}$	11.485(5)	11.147(5)
$c/\text{\AA}$	18.005(5)	17.686(5)
$\beta/^\circ$	133.65(5)	133.30(5)
$V/\text{\AA}^3$	3769(2)	3519(2)
Z	4	4
μ_{Mo}	0.590	0.632
θ range/ $^\circ$	2.10 to 27.63	2.15 to 27.94
Space group	$C2/c$	$C2/c$
$\lambda/\text{\AA}$	0.71069	0.71069
Independent reflections	1320	1725
R^a	0.131	0.128
wR_2^b	0.144	0.136

$$^a R = \sum(|F_o| - |F_c|)/\sum|F_o|. \quad ^b wR_2 = \{\sum[w(F_o^2 - F_c^2)^2]/\sum[w(F_o^2)^2]\}^{1/2}.$$

meters refinement were made through the program SCALEPACK.²⁷ The resulting set of hkl was used for structure solution and refinement. Crystallographic data details on data collections and structure refinements are listed in Table 1.† Structure drawings were carried out with Diamond v3 software.²⁸

The starting structures were solved by direct methods with SIR97.²⁹ The remaining non-hydrogen atoms of the polymeric chains were located by successive difference Fourier map analyses. The hydrogen atoms were placed geometrically and then included in the structure refinement using soft restraints on the bond lengths and angles to regularise their geometry (C–H in the range 0.93–0.98 Å and O–H = 0.82 Å) and isotropic atomic displacement parameters ($U(\text{H})$ in the range 1.2–1.5 times U_{eq} of the adjacent atom). They were then fixed in the final cycles of the refinement with Crystals.³⁰ After the atomic structure of the chains was completed, there still were large cavities where delocalised electronic density was present (maximum residual density of $\sim 2.5 \text{ e } \text{\AA}^{-3}$). Those remaining weak density peaks could thus not be attributed to localised ethanol solvent molecules. The discrete Fourier transform of the observed density in the solvent area was calculated and incorporated as the solvent contribution to the structure factors and refinement procedure through the SQUEEZE algorithm³¹ in PLATON.³² This led to a significant lowering of the reliability factors. The solvent accessible voids found with this procedure are 1030 Å³ and 861 Å³ for the room temperature and low temperature structures, respectively. One can suppose that the high reliability factors found for both structures (see Table 1) are directly related to the nature of the complex. Indeed, several crystals from different batches were recorded and they all showed the same habit: high mosaicity, unstable refinement, disordered solvent. This feature may be caused by crystal lattice defects and variable polymer chain lengths within the crystal. The difference in the coordination geometry of iron(II) inside a chain and at its end, as well as the

† CCDC reference numbers 616015 and 616016. For crystallographic data in CIF or other electronic format see DOI: 10.1039/b608679a

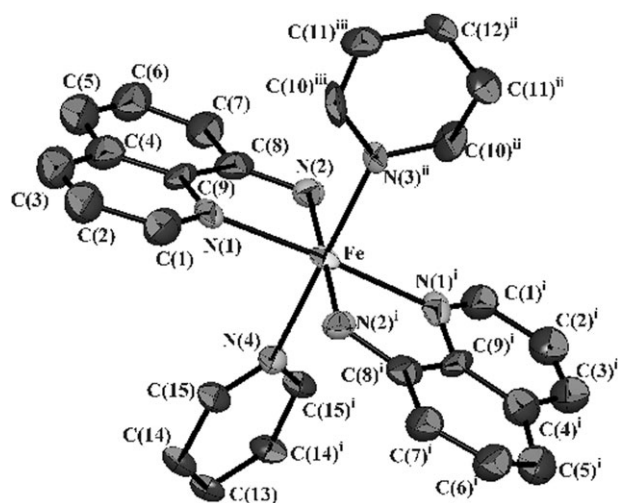


Fig. 1 ORTEP drawing of the local coordination of Fe in the cationic unit structure of $[\text{Fe}(\text{aqin})_2(4,4'\text{-bpy})](\text{ClO}_4)_2 \cdot 2\text{EtOH}$ at 293 K (ellipsoids enclose 30% probability). Only one half of each 4,4'-bpy is shown. The hydrogen atoms are omitted for clarity. ⁱSymmetry operation: $-x, y, 1/2 - z$; ⁱⁱSymmetry operation: $x, 1 + y, z$; ⁱⁱⁱSymmetry operation: $-x, 1 + y, 1/2 - z$.

length dispersion of the chains, can introduce a disorder in the crystal packing. In particular this effect can predominate along the chain axis, thus generating disorder of the solvent and counter-ions position. A clue for this “stacking disorder” was given by the refinement difficulties encountered during the first refining, the atomic positions showing high shifts along the *c* axis of the unit cell.

Results

Description of the structure

The single crystal X-ray structure of $[\text{Fe}(\text{aqin})_2(4,4'\text{-bpy})](\text{ClO}_4)_2 \cdot 2\text{EtOH}$ was determined in the HS (293 K) and LS (80 K) states. Both spin states isomers adopt the monoclinic space group $C2/c$ ($Z = 4$).

The distorted octahedral coordination sphere of the iron(II) atom is formed by six nitrogen atoms belonging to two aqin ligands and two different bifunctional 4,4'-bpy spacers, as can be seen in Fig. 1. In the crystal, the iron atom lies on a twofold rotation axis. The complex assumes a one-dimensional linear

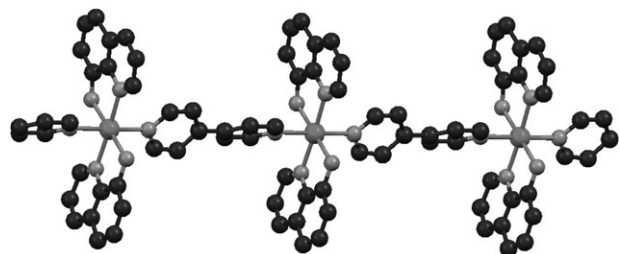


Fig. 2 Linear chain structure of $[\text{Fe}(\text{aqin})_2(4,4'\text{-bpy})](\text{ClO}_4)_2 \cdot 2\text{EtOH}$ at 293 K. The hydrogen atoms and perchlorate ions are omitted for clarity.

Table 2 Selected bond distances (Å) and angles (deg) for $[\text{Fe}(\text{aqin})_2(4,4'\text{-bpy})](\text{ClO}_4)_2 \cdot 2\text{EtOH}$. Estimated standard deviations in the least significant digits are given in parentheses. ⁱ Symmetry operation: $-x, y, 1/2 - z$

	<i>T</i> = 293 K	<i>T</i> = 80 K
Fe–N(1)	2.17(1)	1.96(9)
Fe–N(2)	2.16(1)	2.06(1)
Fe–N(3)	2.20(2)	2.02(1)
Fe–N(4)	2.22(2)	2.01(1)
N(1)–Fe–N(2)	78.5(5)	82.5(5)
N(1)–Fe–N(2) ⁱ	101.4(5)	97.6(5)
N(1)–Fe–N(3)	91.8(3)	92.6(3)
N(1)–Fe–N(4)	88.2(3)	87.4(3)
N(2)–Fe–N(3)	90.6(3)	88.4(3)
N(2)–Fe–N(4)	89.4(3)	91.6(3)
N(1)–Fe–N(1) ⁱ	176.3(6)	174.8(5)
N(2)–Fe–N(2) ⁱ	178.9(6)	176.7(6)
N(3)–Fe–N(4)	180.0(6)	180.0(5)

chain structure, showing the preference of the iron for the *trans*-arrangement of the two 4,4'-bpy ligands (Fig. 2).

Selected bond lengths and angles are given in Table 2.

High-spin complex structure (*T* = 293 K). The Fe–N distances in the coordination polyhedron (see Table 2) are typical of a HS iron(II) complex. The N–Fe–N angles fall within 78.5(5)–101.4(5)° for the adjacent nitrogen atoms and 175.6(3)–180.0(6)° for the opposite ones, instead of 90.00° and 180.00° for an ideal octahedron. The $[\text{FeN}_6]$ core is highly distorted, as revealed by the Σ parameter which is 55.66°. This parameter is defined as the sum of the deviations from 90° of the *cis*-N–Fe–N angles, and gives a quantification of the octahedral distortion of the $[\text{FeN}_6]$ coordination sphere.³³ The distortion of the $[\text{FeN}_6]$ core from O_h is certainly due to steric constraints shoving the bidentate ligands out of the ideal plan. The 4,4'-bpy ligand deviates from planarity, the dihedral angle between the pyridine cycles being 40°.

The polymer linear chains run along the *b* axis. At 293 K, the Fe–Fe distance in a chain is 11.485 Å. The polymer chains are packed in sheets parallel to the *bc* plane, as can be seen in Fig. 3 displaying a projection of the structure on the *ac* plane. The shorter Fe–Fe distance is 9.175 Å for two iron atoms belonging to two neighbouring sheets and 10.171 Å for two iron atoms in two adjacent chains in the same sheet. The chains have alternate orientations (see Fig. 4). The aqin ligands in two adjacent chains are disposed in parallel planes and are thus liable to have π -stacking interactions. Still, the shortest distance between the carbon atoms at HS is 3.74 Å, which is a bit too long for effective π -stacking.

The space between the *bc* sheets is occupied by perchlorate ions (see Fig. 3). Despite a relatively high value of the thermal anisotropic factors, the perchlorate group is resolved in a single orientation. The sheet structure is stabilised by H-bonding of neighbouring chains involving the perchlorate groups and aqin ligands. The ClO_4^- ions also bind adjacent sheets of molecules together *via* H-bonds with aqin and 4,4'-bpy ligands. Detailed information on the hydrogen bonding information is listed in Table 3.

The presence of ethanol molecules in the crystal lattice was revealed by the elemental and thermogravimetric analyses.

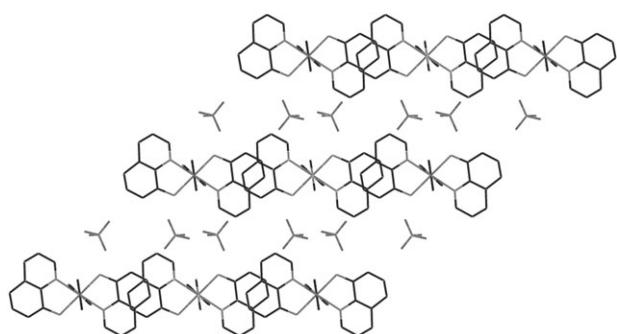


Fig. 3 Projection of the crystal structure of $[\text{Fe}(\text{aqin})_2(4,4'\text{-bpy})](\text{ClO}_4)_2 \cdot 2\text{EtOH}$ on the ac plane, showing the parallel sheets of complex molecules and counter-ions.

However, due to a highly disordered solvent structure, it was impossible to locate them precisely, therefore they are not represented on the structure drawings. The solvent accessible voids are localised between the bc polymer sheets, so that a strong involvement of solvent molecules in intermolecular H-bonding can be expected.

Low-spin complex structure ($T = 80 \text{ K}$). According to the magnetic data, the complex $[\text{Fe}(\text{aqin})_2(4,4'\text{-bpy})](\text{ClO}_4)_2 \cdot 2\text{EtOH}$ presents a predominantly LS form at this temperature. The main structure of the complex is retained upon spin conversion, there is no change in the symmetry space group. The main structural modifications occur in the $[\text{FeN}_6]$ core. The HS \rightarrow LS conversion is accompanied by a shortening of the Fe–N bonds by about 0.2 \AA , which is a typical feature for Fe(II) spin-crossover complexes. The N–Fe–N angles fall in a $87.4(3)\text{--}97.6(5)^\circ$ and $174.8(5)\text{--}180.0(5)^\circ$ range. On cooling the Fe–Fe distances become shorter than at room temperature and are equal to 11.147 \AA for two neighbouring iron atoms in a chain, 8.980 \AA for two iron atoms in two neighbouring sheets and 10.007 \AA for two atoms in neighbouring chains in the same sheet.

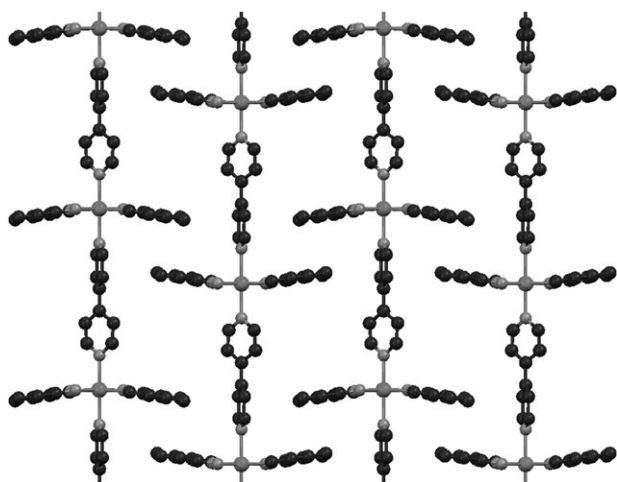


Fig. 4 Projection of the crystal structure of $[\text{Fe}(\text{aqin})_2(4,4'\text{-bpy})](\text{ClO}_4)_2 \cdot 2\text{EtOH}$ in the $[100]$ plane. The hydrogen atoms and perchlorate ions are omitted for clarity.

Table 3 Interatomic distances (\AA) and angles ($^\circ$) for the hydrogen bonding interactions for $[\text{Fe}(\text{aqin})_2(4,4'\text{-bpy})](\text{ClO}_4)_2 \cdot 2\text{EtOH}$. Estimated standard deviations in the least significant digits are given in parentheses

D–H...A	D–H	H...A	D...A	D–H...A
293 K				
N ₂ –H ₂₁ ...O ₁	0.89	2.441	3.24(3)	150.9
C3–H ₃₁ ...O ₁	0.93	2.504	3.33(4)	148.5
C ₁₀ –H ₁₀₁ ...O ₄	0.93	2.605	3.29(2)	131.0
80 K				
N ₂ –H ₂₁ ...O ₁	1.00	2.628	3.47(2)	141.6
N ₂ –H ₂₁ ...O ₂	1.00	2.339	3.27(1)	154.0
C ₃ –H ₃₁ ...O ₁	0.93	2.345	3.21(3)	153.4
C ₁₀ –H ₁₀₁ ...O ₄	0.93	2.618	3.27(3)	127.6

The unit cell volume decreases by 250 \AA^3 or 6.63% upon the spin conversion. On cooling the anisotropy of the unit cell contraction is respectively, 2.62, 2.94 and 1.77% for the a , b and c axes. The crystal packing is similar to that in the HS state. The pattern of hydrogen bonding with the perchlorate anions is retained, however the intermolecular π -stacking interactions within a bc sheet become slightly stronger, the shortest distance between two carbon atoms being 3.62 \AA .

Magnetic susceptibility data

The magnetic properties of the complex are represented in Fig. 5 in the form of a $\chi_M T$ versus T plot, χ_M being the molar magnetic susceptibility. At 293 K, $\chi_M T$ is equal to $3.53 \text{ cm}^3 \text{ mol}^{-1} \text{ K}$, which corresponds to a quintet spin state. This value decreases gradually upon cooling to 250 K and then descends more abruptly to 190 K. The spin conversion temperature $T_{1/2}$ is found at 220 K. The weak paramagnetism at low temperature ($\chi_M T = 0.13 \text{ cm}^3 \text{ mol}^{-1} \text{ K}$ at $T = 80 \text{ K}$) can be related to temperature-independent paramagnetism. No thermal hysteresis was observed.

The thermodynamic parameters of the spin transition were obtained using the regular solution model of Schlichter and Drickamer,³⁴ which leads to the following equation for the HS molecular fraction γ_{HS}

$$\ln[(1 - \gamma_{\text{HS}})/\gamma_{\text{HS}}] = [\Delta H + \Gamma(1 - 2\gamma_{\text{HS}})]/RT - \Delta S/R$$

where ΔH and ΔS are the enthalpy and entropy variations associated with the spin transition, and Γ the interaction parameter characterising cooperativity. The residual HS fraction at low temperature was excluded from the iterative relative-error minimisation routine. Fig. 5 illustrates the simulated spin-crossover behaviour of the complex with parameters $\Delta H = 14.7 \text{ kJ mol}^{-1}$, $\Delta S = 66.8 \text{ J mol}^{-1} \text{ K}^{-1}$ and $\Gamma = 1.8 \text{ kJ mol}^{-1}$. The agreement factor defined as $\sum_i [(\chi_M T)_{i,\text{exp}} - (\chi_M T)_{i,\text{calc}}]^2 / \sum_i [(\chi_M T)_{i,\text{exp}}]^2$ is 1×10^{-3} . The calculated thermodynamic parameters are close to those usually observed for iron(II) spin-crossover compounds.

Discussion

The complex $[\text{Fe}(\text{aqin})_2(4,4'\text{-bpy})](\text{ClO}_4)_2 \cdot 2\text{EtOH}$ discussed here represents one of the rare examples of structurally characterised polymeric spin-crossover complexes and the first polymer using the 8-aminoquinoline ligand. The synthesis of this product illustrates the utility of the strategy introduced in

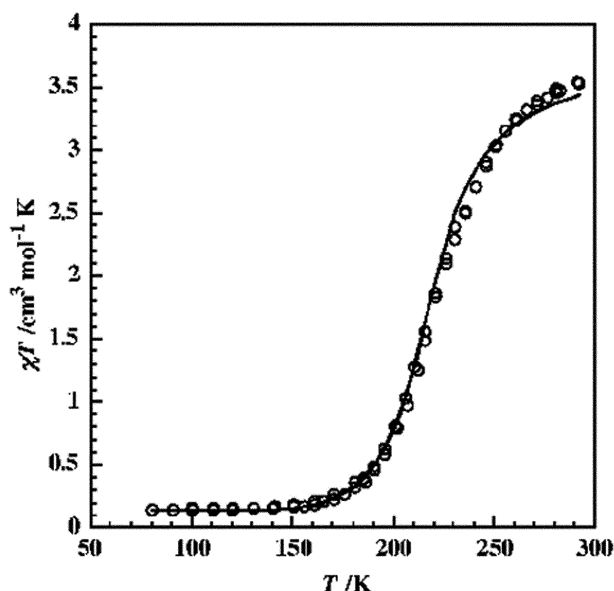


Fig. 5 Thermal variation of $\chi_M T$ (circles) and fitting (plain line) for $[\text{Fe}(\text{aqin})_2(4,4'\text{-bpy})](\text{ClO}_4)_2 \cdot 2\text{EtOH}$.

ref. 18 and 24, which is based on self-assembly of organic molecules with functionally distinct types of nitrogen donor atoms and metal ion building blocks for the synthesis of new polynuclear spin transition systems. Although the localisation of the solvent molecules by X-ray diffraction met important difficulties, the structure of the polymeric network has been unambiguously resolved. It displays linear chains in which the iron(II) sites are directly linked to each other by the rigid rodlike 4,4'-bipyridine molecule, whereby the intersite interactions may be efficiently spread. The coordination polyhedron of the iron(II) site is completed in octahedral geometry by two bidentate 8-aminoquinoline ligands. The magnetic measurements for this compound reveal a relatively abrupt spin transition with $T_{1/2} = 220$ K. The absolute value of the cooperativity parameter $\Gamma = 1.8$ kJ mol⁻¹, found from the fitting procedure with the regular solution model, is indicative of the systems exhibiting cooperative effects. However, according to the Schlichter and Drickamer model the value of the cooperativity parameter for which a hysteresis effect must be observed is higher and equal to $2RT_{1/2} = 3.65$ kJ mol⁻¹. Different structural characteristics of the complex can account for the cooperativity of the system. The first one is the rigidity of the ligand linking the metallic centers. The Fe–Fe separation *via* the 4,4'-bpy ligand is equal to 11.485 Å in the HS structure. The polymeric chains that extend along the *b* axis are stacked in *bc* sheets. Slight interchain π -stacking interactions can also contribute to the cooperativity of the spin transition. This particular structural arrangement allows the intermolecular Fe–Fe distances to be shorter than the intramolecular one. The adjacent polymeric chains are bound to one another by H-bonds involving the oxygen atoms of the perchlorate anions and amino groups of aqin ligands directly linked to the metal sites. The neighbouring sheets in the *a* direction are also linked by H-bonds between the perchlorate ions and the 4,4'-bpy ligands. Moreover, it is very likely that

the two molecules of crystallisation ethanol also participate in the H-bonding, and thus play a role in enhancing the interactions between the metal sites. All these features can account for rather strong interactions between the metal centers that lead to cooperative effects.

Only two polymeric spin-crossover complexes with linear chains have been reported in literature until now. The first one, *catena*- $[\mu\text{-tris}(1,2\text{-bis}(\text{tetrazol-1-yl})\text{propane-N1,N1'})\text{iron(II)}](\text{ClO}_4)_2$, forms linear chains that run along the *c* axis, in which the iron atoms are separated by 7.4 Å at HS.¹⁴ The chains are packed in such a way that channels appear between them, where the noncoordinated perchlorate anions are located. Magnetic susceptibility measurements reveal a very gradual incomplete spin transition with $T_{1/2} = 130$ K. The low grade of cooperativity can be attributed to the flexibility of the 1,2-bis(tetrazol-1-yl)ethane ligand, leading to a “shock-absorber” effect which does not allow elastic interactions to be transmitted efficiently from one magnetic center to the other. The second one, $[\text{Fe}(4,4'\text{-4,4'-bpy})(\text{bt})(\text{NCS})_2]$ (bt = 2,2'-bithiazoline) displays a linear chain structure with close Fe–Fe separation *via* the 4,4'-bpy ligand (11.145 Å).¹⁸ This complex displays an incomplete and gradual HS \leftrightarrow LS conversion. There is no reported information on intramolecular H-bonds or π -stacking interactions.

Comparing with previous examples, we can note that the spin-transition in the presented linear polymer $[\text{Fe}(\text{aqin})_2(4,4'\text{-bpy})](\text{ClO}_4)_2 \cdot 2\text{EtOH}$ is complete and more cooperative.

Another example of a polymer using the 4,4'-bpy spacer is represented by $[\text{Fe}(\text{pyim})_2(4,4'\text{-bpy})](\text{ClO}_4)_2 \cdot 2\text{EtOH}$ (where pyim = 2-(2-pyridyl)imidazole), in which the *cis* coordination of the 4,4'-bpy molecules leads to a one-dimensional zigzag-chain structure.²⁴ This complex exhibits a rather abrupt spin-transition with $T_{1/2} = 205$ K. Although the chains are not linear, this complex shares several features with $[\text{Fe}(\text{aqin})_2(4,4'\text{-bpy})](\text{ClO}_4)_2 \cdot 2\text{EtOH}$. The intrachain Fe–Fe distances are 11.523 Å for the HS form and 11.201 Å for the LS form, close to what is observed with $[\text{Fe}(\text{aqin})_2(4,4'\text{-bpy})](\text{ClO}_4)_2 \cdot 2\text{EtOH}$. The chains arrange in sheets of molecules in which they are linked by π -stacking, the shortest Fe–Fe interchain distance being 9.110 Å at high-spin and 8.994 Å at low-spin. There are also strong intermolecular H-bonding through the perchlorate anions and the solvent molecules. The $[\text{Fe}(\text{aqin})_2(4,4'\text{-bpy})](\text{ClO}_4)_2 \cdot 2\text{EtOH}$ and $[\text{Fe}(\text{pyim})_2(4,4'\text{-bpy})](\text{ClO}_4)_2 \cdot 2\text{EtOH}$ complexes thus have resembling intermolecular interactions and display rather similar magnetic properties. An enhanced conjugation in the aqin ligand compared with pyim makes the ligand field a bit stronger and heightens $T_{1/2}$.

Bipyridine-like spacers have also led to two other spin-crossover compounds. $[\text{Fe}(\text{tvp})_2(\text{NCS})_2] \cdot \text{CH}_3\text{OH}$ (tvp = 1,2-di-(4-pyridyl)ethylene) represents the first catenane supramolecular system showing the occurrence of two perpendicular, fully interlocked two-dimensional networks (Fe–Fe = 13.66 Å).¹³ Nevertheless, the spin transition has a gradual and incomplete character, depending also on sample preparation. There is no information regarding intermolecular H-bonding or π -stacking. The second complex $[\text{Fe}(\text{bpb})_2(\text{NCS})_2] \cdot 0.5\text{MeOH}$ (bpb = 1,4-bis(4-pyridyl)butadiene) is a singular example of the interpenetration of three mutually

perpendicular nets.¹⁵ It displays a 50% gradual spin conversion related to the presence of two iron(II) sites in the crystal lattice. The Fe–Fe separation at two sites through the bpb ligand are 16.628 and 16.313 Å. No intermolecular interactions are reported.

The aforesaid examples demonstrate that the building of polymers with rodlike spacers directly linking iron(II) atoms can be a promising road toward new spin transition materials. They clearly indicate however that the Fe–Fe distance alone does not determine the cooperativity of the spin transition, and that the mere direct linking of active sites is not a sufficient condition to generate highly cooperative systems. The presence of effective π -stacking and/or H-bonding and the rigidity of the chemical bridges efficiently spreading the intermolecular interactions are important parameters governing the steepness of the spin-crossover. So, the ligands containing amino groups liable to take part in intermolecular H-bonding are of particular interest for the design of cooperative systems. The results obtained with [Fe(aqin)₂(4,4'-bpy)](ClO₄)₂·2EtOH are encouraging in this sense. They show that choosing ligands that can favor intermolecular interactions as building blocks constitutes a promising way toward new highly cooperative spin-crossover systems.

Acknowledgements

The authors thank Stéphanie Calmettes for the thermogravimetric measurements. We are grateful to Serguei Borshch for helpful discussion. This work was supported by the EU through NE MAGMANET (FP6-NMP3-CT-2005-515767).

References

- 1 *Spin Crossover in Transition Metal Compounds I–III*, ed. P. Gülich and H. A. Goodwin, in Topics in Current Chemistry, 2004, vol. 233–235.
- 2 (a) P. Gülich, *Struct. Bonding (Berlin)*, 1981, **44**, 83; (b) P. Gülich, A. Hauser and H. Spiering, *Angew. Chem., Int. Ed. Engl.*, 1994, **33**, 2024; (c) H. Toftlund, *Coord. Chem. Rev.*, 1989, **94**, 67; (d) E. König, G. Ritter and S. K. Kulshreshtha, *Chem. Rev.*, 1985, **85**, 219; (e) E. König, *Struct. Bonding (Berlin)*, 1991, **76**, 51; (f) J. Zarembowitch and O. Kahn, *New J. Chem.*, 1991, **15**, 181; (g) O. Kahn, *Molecular Magnetism*, Wiley VCH, New York, 1993; (h) J. A. Real, in *Transition Metals in Supramolecular Chemistry*, ed. J.-P. Sauvage, Wiley, New York, 1999; (i) J. A. Real, A. B. Gaspar and M. C. Muñoz, *Dalton Trans.*, 2005, 2062.
- 3 (a) O. Kahn and J.-P. Launay, *Chemtronics*, 1988, **3**, 140; (b) O. Kahn, J. Kröber and C. Jay, *Adv. Mater.*, 1992, **4**, 718; (c) J.-F. Létard, P. Guionneau and L. Goux-Capes, *Top. Curr. Chem.*, 2004, **235**, 221.
- 4 J. A. Real, A. B. Gaspar, V. Niel and M. C. Muñoz, *Coord. Chem. Rev.*, 2003, **236**, 121.
- 5 (a) G. S. Matouzenko, A. Bousseksou, S. Lecocq, P. J. van Koningsbruggen, M. Perrin, O. Kahn and A. Collet, *Inorg. Chem.*, 1997, **36**, 5869; (b) G. S. Matouzenko, J.-F. Létard, A. Bousseksou, S. Lecocq, L. Capès, L. Salmon, M. Perrin, O. Kahn and A. Collet, *Eur. J. Inorg. Chem.*, 2001, **11**, 2935; (c) G. S. Matouzenko, A. Bousseksou, S. A. Borshch, M. Perrin, S. Zein, L. Salmon, G. Molnár and S. Lecocq, *Inorg. Chem.*, 2004, **43**, 227.
- 6 (a) O. Kahn and E. Codjovi, *Philos. Trans. R. Soc. London, Ser. A*, 1996, **354**, 359; (b) O. Kahn, Y. Garcia, J.-F. Létard and C. Mathonière, *NATO ASI Ser., Ser. C*, 1998, **518**, 127.
- 7 (a) H. W. Roesky and M. Andruh, *Coord. Chem. Rev.*, 2003, **236**, 91; (b) M. Zaworotko, *Chem. Commun.*, 2001, 1.
- 8 C. Chen and K. S. Suslick, *Coord. Chem. Rev.*, 1993, **128**, 293, and references therein.
- 9 Y. Garcia, V. Niel, M. C. Muñoz and J. A. Real, *Top. Curr. Chem.*, 2004, **233**, 229.
- 10 W. Vreugdenhil, J. H. Van Diemen, R. A. G. de Graaff, J. G. Haasnoot, J. Reedijk, A. M. van der Kraan, O. Kahn and J. Zarembowitch, *Polyhedron*, 1990, **9**, 2971.
- 11 O. Kahn and C. J. Martinez, *Science*, 1998, **279**, 44.
- 12 Y. Garcia, O. Kahn, L. Rabardel, B. Chansou, L. Salmon and J.-P. Tuchagues, *Inorg. Chem.*, 1999, **38**, 4663.
- 13 J. A. Real, E. Andrés, M. C. Muñoz, M. Julve, T. Granier, A. Bousseksou and F. Varret, *Science*, 1995, **268**, 265.
- 14 P. J. van Koningsbruggen, Y. Garcia, O. Kahn, L. Fournès, H. Kooijman, A. L. Spek, J. G. Haasnoot, J. Moscovici, K. Provost, A. Michalowicz, F. Renz and P. Gülich, *Inorg. Chem.*, 2000, **39**, 1891.
- 15 N. Moliner, M. C. Muñoz, S. Létard, X. Solans, N. Menéndez, A. Goujon, F. Varret and J. A. Real, *Inorg. Chem.*, 2000, **39**, 5390.
- 16 J. Schweifer, P. Weinberger, K. Mereiter, M. Boca, C. Reichl, G. Weisinger, G. Hilscher, P. J. van Koningsbruggen, H. Kooijman, M. Grunert and W. Linert, *Inorg. Chim. Acta*, 2002, **339**, 297.
- 17 J. Kröber, E. Codjovi, O. Kahn, F. Grolrière and C. Jay, *J. Am. Chem. Soc.*, 1993, **115**, 9810–9811.
- 18 N. Moliner, M. C. Muñoz, S. Létard, L. Salmon, J.-P. Tuchagues, A. Bousseksou and J. A. Real, *Inorg. Chem.*, 2002, **41**, 6997.
- 19 K. Abu-Shandi, H. Winkler, H. Paulsen, R. Glaum, B. Wu and C. Janiak, *Z. Anorg. Allg. Chem.*, 2005, **631**, 2705.
- 20 O. Roubeau, J. M. Alcazar Gomez, E. Balskus, J. J. A. Kolnaar, J. G. Haasnoot and J. Reedijk, *New J. Chem.*, 2001, **25**, 144.
- 21 P. Rosa, A. Debay, L. Capes, G. Chastanet, A. Bousseksou, P. Le Floch and J.-F. Létard, *Eur. J. Inorg. Chem.*, 2004, **2004**, 3017.
- 22 C. M. Grunert, J. Schweifer, P. Weinberger and W. Linert, *Inorg. Chem.*, 2004, **43**, 155.
- 23 Y. Garcia, G. Bravic, C. Gieck, D. Chasseau, W. Tremel and P. Gülich, *Inorg. Chem.*, 2005, **44**, 9723–9730.
- 24 G. S. Matouzenko, G. Molnár, N. Bréfuel, M. Perrin, A. Bousseksou and S. A. Borshch, *Chem. Mater.*, 2003, **15**, 550.
- 25 K. Yoneda, K. Adachi, S. Hayami, Y. Maeda, M. Katada, A. Fuyuhiko, S. Kawata and S. Kaizaki, *Chem. Commun.*, 2006, 45.
- 26 Nonius, *COLLECT*, Nonius BV, Delft, The Netherlands, 1997–2001.
- 27 Z. Otwinowski and W. Minor, *Methods Enzymol.*, 1997, **276**, 307.
- 28 K. Brandenburg and H. Putz, *DIAMOND*, Crystal Impact GbR, Postfach 1251, D-53002 Bonn, Germany, 1996.
- 29 A. Altomare, M. C. Burla, M. Camalli, G. L. Cascarano, C. Giacovazzo, A. Guagliardi, A. Moliterni, G. Polidori and R. Rizzi, *J. Appl. Crystallogr.*, 1999, **32**, 115.
- 30 P. W. Betteridge, J. R. Carruthers, R. I. Cooper, K. Prout and D. J. Watkin, *J. Appl. Crystallogr.*, 2003, **36**, 1487.
- 31 P. van der Sluis and A. L. Spek, *Acta Crystallogr., Sect. A: Fundam. Crystallogr.*, 1990, **46**, 194.
- 32 A. L. Spek, *Acta Crystallogr., Sect. A: Fundam. Crystallogr.*, 1990, **46**, C34.
- 33 P. Guionneau, C. Brigouleix, Y. Barrans, A. E. Goeta, J.-F. Létard, J. A. K. Howard, J. Gaultier and D. Chasseau, *C. R. Acad. Sci., Ser. IIc: Chim.*, 2001, **4**, 161.
- 34 C. P. Schlichter and H. G. Drickamer, *J. Chem. Phys.*, 1972, **56**, 2142.